![AIAA logo]

AIAA-2001-2005
Computer Simulation of Parafoil Dynamics

Yan Zhu, Melissa Moreau, Michael Accorsi, and John Leonard
University of Connecticut
Storrs, CT

John Smith
Pioneer Aerospace Corporation
South Windsor, CT

16th AIAA Aerodynamic Decelerator Systems Technology Conference
22-24 May 2001
Boston, Massachusetts

Computer Simulation of Parafoil Dynamics

Yan Zhu, Melissa Moreau, Michael Accorsi, John Leonard
Department of Civil and Environmental Engineering
University of Connecticut, Storrs, CT 06269-2037
yanz@engr.uconn.edu, moreau@engr.uconn.edu, accorsi@engr.uconn.edu, leonard@engr.uconn.edu

John Smith
Pioneer Aerospace Corporation
South Windsor, CT 06074
jsmith@pioneeraero.com

Abstract

Three-dimensional transient simulations of unconstrained flight of a parafoil system are performed using a structural finite element model with prescribed pressure and drag forces. In general, simulation of parafoil flight requires coupling of a structural model with a fluid dynamics model. The approach presented here is an intermediate step towards a fully-coupled simulation. Since the structural model is considerably smaller than the required fluid dynamics model, these intermediate simulations are considerably easier to perform and provide a relatively simple method to evaluate parafoil flight. Simulations of the inflation from the initial cut pattern, steady glide, and turning and flared landing maneuvers are presented.

Introduction

Parafoils are a unique type of parachute system that provide high glide capability due to their wing type geometry. Parafoils have been used for a variety of applications where delivery accuracy is critical with payloads ranging from light (200 lb) to heavy (15,000 lb). Due to the complex aerodynamic behavior of parafoils, they are typically designed using semi-empirical methods[1] supplemented with extensive testing. This approach to design is time consuming and expensive and therefore additional design tools are desirable.

Computer simulation of parachute systems has advanced significantly in the last five years. In general, these simulations require coupling of a structural dynamics (SD) model for the parachute and suspension lines with a fluid dynamics (FD) model for the surrounding air flow. Useful results, however, can be obtained from either a stand-alone SD simulation with prescribed fluid loads or a stand-alone FD simulation with prescribed canopy geometry.

Tezduyar *et al*[2] have performed stand-alone FD simulations of the flow around a parafoil canopy with prescribed geometry. Ibos *et al*[3] have performed coupled simulations of a parafoil in its steady glide configuration. Benney *et al*[4] have performed stand-alone simulations of an unconstrained parafoil in steady glide. Chatzikonstantinou[5] has identified the numerous difficulties encountered in performing such simulations.

The SD and FD models are both nonlinear and time-dependent. The SD model only requires a computational mesh over the surface of the canopy and suspension lines. The FD model requires a mesh over the volume of fluid surrounding the parafoil to an outer boundary where the flow is essentially undisturbed. Therefore, the FD model is considerably larger than the SD model.

In this paper, we present intermediate methods to simulate the flight and control of parafoils. Specifically, we develop methods to approximate the fluid loads to allow for meaningful stand-alone structural simulations. The goal of these intermediate methods is to provide realistic simulations without requiring a large-scale computational fluid dynamics model. These intermediate methods provide quick results that are suitable for preliminary evaluation of parafoil systems.

Four types of simulations on parafoil systems are performed that include (1) inflation from a cut pattern, (2) 3D unconstrained steady glide, (3) 3D unconstrained turning maneuvers, and (4) flared landing maneuvers.

Structural Model Generation

The first step in these simulations is to generate a structural finite element model for parafoil systems. Our goal in this step was to develop a general tool that could automatically generate different models to allow for the evaluation of many systems with potential design changes.

The automatic parafoil model generator follows five steps:

1. The rib is divided into geometric units (8 point quadrilateral and 6 point triangular) as shown in Figure 1. Rib reinforcements can be included along the edges of the geometric units.
2. The rib is subdivided into triangular membrane elements using a specified level of refinement as shown in Figure 2.
3. Floor and roof panels are generated to match the rib, and all parts are duplicated for a specified number of cells.
4. Suspension line patterns are used to generate cable elements that are attached to the canopy model as shown in Figure 3.
5. Canopy reinforcements are modeled as cable elements attached to the corresponding canopy membrane elements. Reinforcement through the rib, along the floor and roof chords, and across the leading edge are shown in Figure 4.

The canopy model that is generated corresponds to the unstressed cut pattern. The suspension lines in this configuration may be taut, slack, or at their true unstressed length. The model generator outputs the true length as well as the nodal coordinates for each cable element to the SD analysis code. This model corresponds to a 420 ft² Genesis parafoil with a 400 pound payload. The finite element model has a total of 7,527 elements with 5804 membrane elements for the canopy, 1,602 cable elements for the canopy reinforcements, 120 cable elements for the suspension lines, and 1 truss element for the payload. The model has 4,552 nodes corresponding to 13,656 degrees of freedom.

Parafoil Structural Modeling

The parafoil canopy and suspension lines are modeled using membrane and cable elements within a geometrically nonlinear, transient, finite element code (TENSION) that has been specialized for simulation of parachute systems. The theoretical foundations of this code have been presented by Accorsi et al [6]. Application of the code to parachute simulations has been presented by Benney et al [7].

The fluid forces on the structural model are approximated by prescribed pressure fields on the floor and roof membranes and velocity dependent drag on canopy cables, suspension lines and payload. The four pressure fields that are used are shown in Figure 5 and correspond to uniform pressures along the floor and roof (p_1 and p_2), and leading edge pressures on the floor and roof (p_3 and p_4). The magnitudes of the pressure fields are calibrated to satisfy dynamic equilibrium for typical steady state flight data.

The forces acting on the structural model in two-dimensional steady flight are the pressure resultants, drag resultants, and payload weight, as shown in Figure 6. For this state, three dynamic equilibrium equations are needed ($\Sigma F_x = \Sigma F_z = \Sigma M_y = 0$). The equilibrium equations are written using a pressure coefficient for the four prescribed pressure fields. For equilibrium of forces in the x direction

$$A_{x1}\, p_1 \;+\; A_{x2}\, p_2 \;+\; A_{x3}\, p_3 \;+\; A_{x4}\, p_4 \;+\; D_x \;=\; 0$$

where the A's are the x-component pressure coefficients corresponding to unit pressure fields and D_x is the total x-component drag resultant due to canopy cables, suspension lines, and payload. Similar equations are written for the remaining two dynamic equilibrium equations. Since there are four pressure fields and only three equations, the value of p_1 is prescribed and the three remaining pressure magnitudes are determined by satisfying equilibrium. Therefore, the equilibrium equations are written as

$$\begin{bmatrix} A_{x2} & A_{x3} & A_{x4} \\ A_{z2} & A_{z3} & A_{z4} \\ A_{y2} & A_{y3} & A_{y4} \end{bmatrix} \begin{Bmatrix} p_2 \\ p_3 \\ p_4 \end{Bmatrix} = \begin{Bmatrix} -D_x - A_{x1}\, p_1 \\ -D_z - A_{z1}\, p_1 + W \\ -D_y - A_{y1}\, p_1 \end{Bmatrix}$$

where W is the payload weight.

The structural model is calibrated by prescribing a steady state configuration (angle of attack and velocity) and extracting the pressure coefficients and drag resultants from the finite element results. Once calibrated, these values are used for all remaining simulations. For the current work, a total velocity of 38

fps with horizontal velocity of 33.3 fps and vertical velocity of 18.3 fps was used for calibration. A chord angle for the parafoil of 4 degrees corresponding to an angle of attack of 24 degrees was also used for calibration. The calibration is performed using this data with only one time step and therefore is easy to execute. The corresponding resultant forces can be calculated after performing the calibration. For the current work, the pressure resultants in the x and z directions are -197 pounds and +153 pounds, respectively. The corresponding drag resultants in the x and z directions are +197 pounds and +247 pounds, respectively.

Parafoil Simulations

Inflation

The true inflation of a parafoil under realistic conditions is extremely complex and difficult to model. Here, we simply model the transition from the unstressed cut pattern (Figure 3) to an inflated shape to obtain a stressed configuration for the remaining simulations. The inflated configuration is shown in Figure 7. Although the inflated shape is intuitively correct, the angle of attack and velocities of this configuration do not correspond to the steady glide state.

Steady Glide

The steady glide simulations begin with the inflated configuration (corresponding to an arbitrary angle of attack and velocities) and use the pressure fields determined above to satisfy two-dimensional dynamic equilibrium. Plots of the parafoil center section (i.e. stick figures) at multiple times are given in Figure 8 and clearly show the transition from an arbitrary starting condition to a well defined steady glide. The horizontal and vertical components of the payload velocity as a function of time are shown in Figure 9 along with the velocity values used for model calibration (horizontal lines). At the starting time, the payload undergoes some extreme motion, then stabilizes at values very close to the calibration values. This demonstrates that the model is able to find its equilibrium state from some arbitrary starting point. The angle of attack and parafoil angle (the angle between the center rib chord and horizontal) are shown in Figure 10 with their calibration values. In Figures 11, 12, and 13 the x-force, z-force, and y-moment resultants and their calibration values are shown as a function of time, respectively. These plots include the pressure resultant, drag resultant, and the total fluid force (pressure plus drag). The total x-force and y-moment approach zero for steady state while the total z-force approaches the system weight.

Turning Maneuver

A turning maneuver is initiated from the steady glide state by shortening one of the two control lines attached to the suspension lines along the trailing edge. The deformed configuration of the structural model during the turn is shown in Figure 14. The depressed trailing edge flap on one side and slight banking motion are apparent. Figure 15 shows multiple stick figure plots of the three-dimensional parafoil trajectory during the turn maneuver. For this case, the parafoil achieves a turning radius of approximately 200 ft. with an angular velocity of 7.5 degrees per second.

Flared Landing Maneuver

A flared landing maneuver is initiated from the steady glide state by shortening both of the control lines attached to the suspension lines along the trailing edge. The deformed configuration of the parafoil in its flared configuration with both trailing edge flaps depressed is shown in Figure 16. The horizontal and vertical velocities of the parafoil during the flare maneuver are shown in Figure 17 along with the respective steady glide velocities. It is seen that the velocities are reduced considerably during the flare maneuver. For this simulation, the total velocity is reduced from an initial value of 38 fps to a final value of 25 fps. Figure 18 shows the parafoil angle and angle of attack during the flare maneuver. The parafoil angle changes from +4 degrees prior to the flare to -10 degrees after the flare.

Conclusions

An intermediate method is presented to model the dynamics of parafoils using a structural finite element model with prescribed fluid forces. The fluid forces are calibrated to a specific flight condition (velocity and angle of attack) by imposing the appropriate equilibrium conditions. It was shown that starting from an arbitrary configuration, the parafoil will reach this equilibrium configuration. In the current work, only one calibration state was used. Since the calibration is easy to execute, multiple calibrations could be performed for a specific model for various flight conditions and stored as a database for that model.

References

1. S. Lingard, "Ram-Air Parachute Design," 13ᵗʰ AIAA Aerodynamic Decelerator Systems Technology Conference, Clearwater, 1995.

2. T. Tezduyar, V. Kalro and W. Garrard, "Advanced Computational Methods for 3D Simulation of Parafoils," 15ᵗʰ CEAS/AIAA Aerodynamic Decelerator Systems Technology Conference, AIAA-1999-1712, Toulouse, 1999.

3. C. Ibos, C. Lacroix, P. Bordenave, L. Chuzet and A. Goy, "Fluid-Structure Simulation of a 3D Ram-Air Parachute with SINPA Software," 15ᵗʰ CEAS/AIAA Aerodynamic Decelerator Systems Technology Conference, AIAA-1999-1713, Toulouse, 1999.

4. R. Benney, K. Stein, J. Leonard, M. Accorsi, "Current 3-D Structural Dynamic Finite Element Modeling Capabilities," 14ᵗʰ AIAA Aerodynamic Decelerator Systems Technology Conference, AIAA-1997-1506, San Francisco, 1997.

5. T. Chatzikonstantinou, "Problems in Ram Air Wing Modeling and Their Solution in the Three Dimensional Simulation Code "PARA3D", 15ᵗʰ CEAS/AIAA Aerodynamic Decelerator Systems Technology Conference, AIAA-1999-1716, Toulouse, 1999.

6. M. Accorsi, J. Leonard, R. Benney and K. Stein, "Structural Modeling of Parachute Dynamics," *AIAA Journal*, 38 (2000) 139-146.

7. R. Benney, K. Stein, W. Zhang, M. Accorsi and J. Leonard, "Controllable Airdrop Simulations Utilizing a 3-D Structural Dynamics Model," 15ᵗʰ CEAS/AIAA Aerodynamic Decelerator Systems Technology Conference, AIAA-1999-1727, Toulouse, 1999.
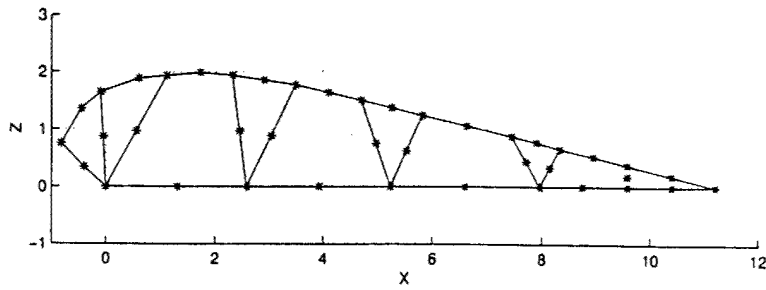
Figure 1: Rib Geometric Units
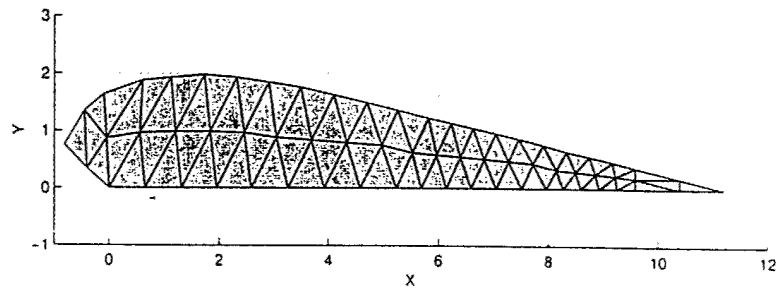
Figure 2: Rib Finite Element Model
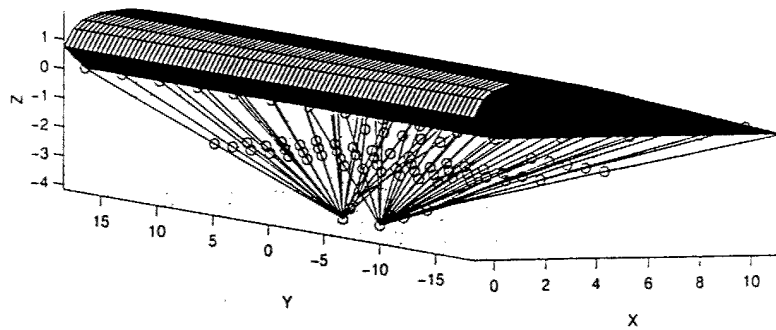
Figure 3: Parafoil Finite Element Model (Cut Pattern)
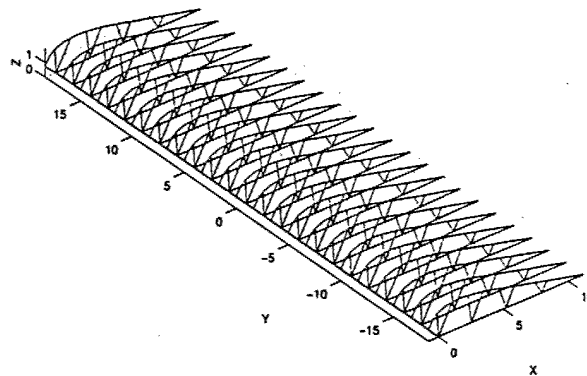
Figure 4: The Canopy Cables

American Institute of Aeronautics and Astronautics
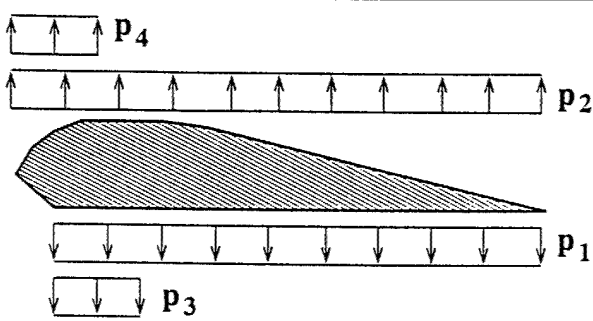
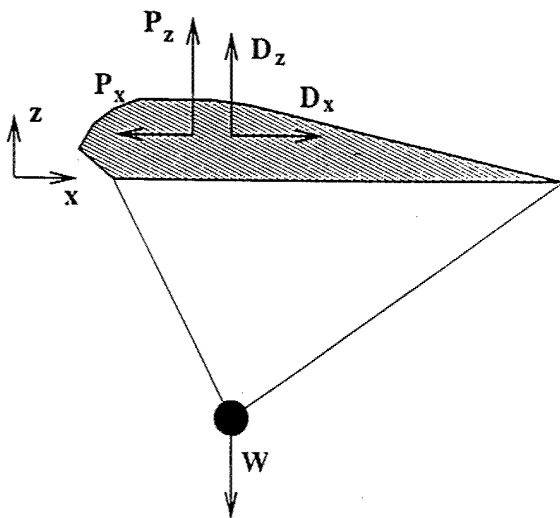Figure 5: Canopy Pressure Distributions

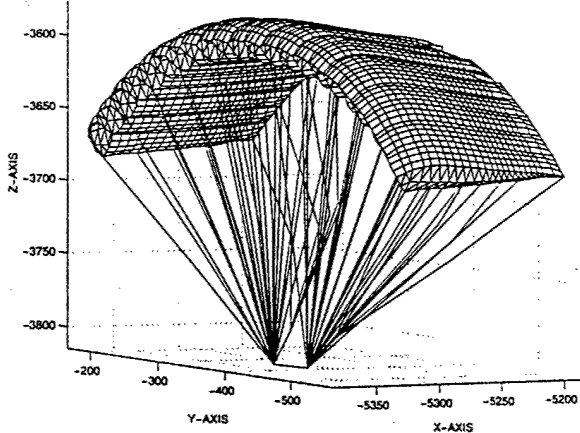
Figure 6: Parafoil Resultant Forces
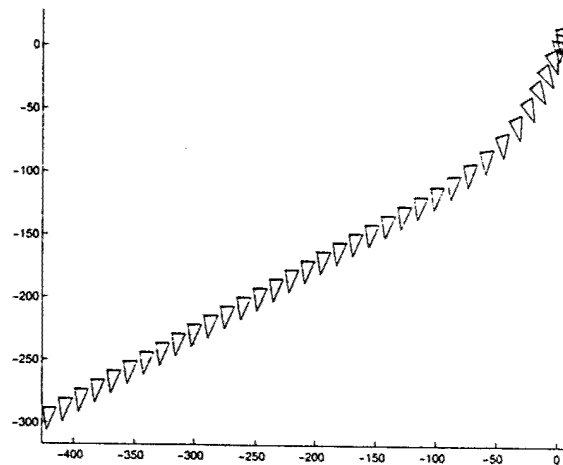

Figure 7: Inflated Parafoil Model
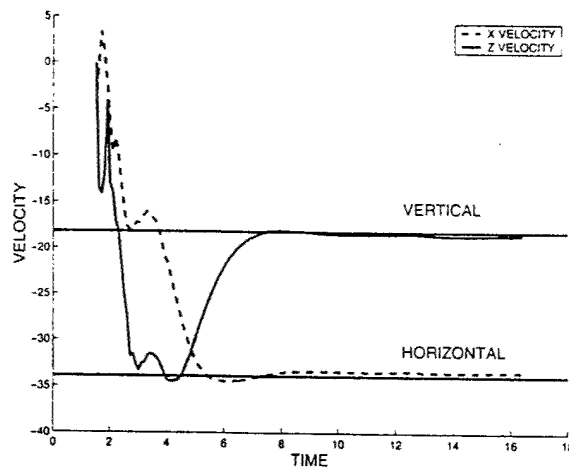

Figure 8: Steady Glide Trajectory
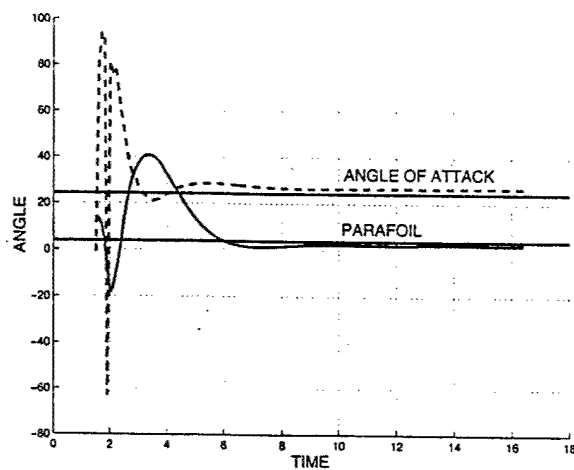

Figure 9: Horizontal and Vertical Velocity
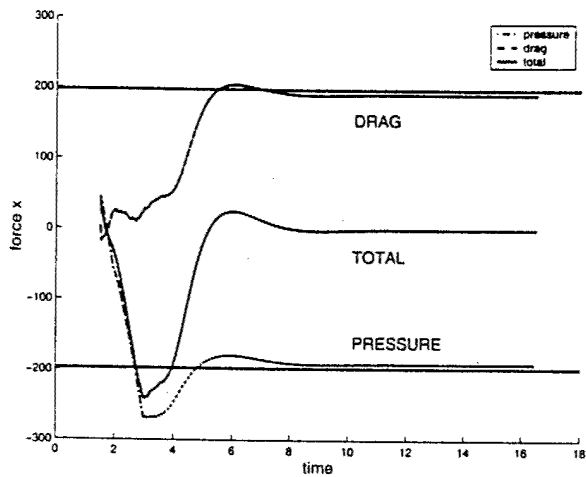

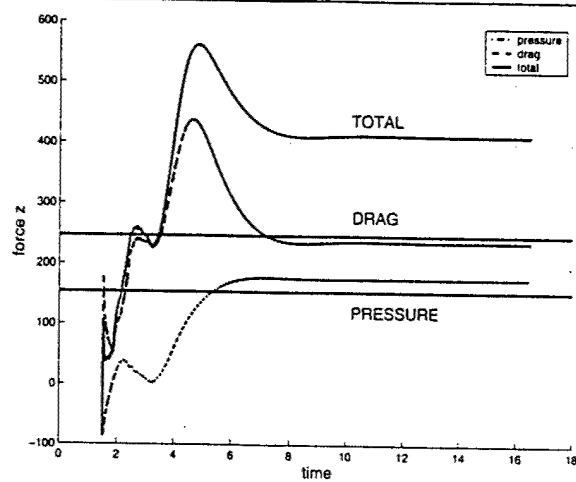Figure 10: Parafoil Angle and Angle of Attack

6

Figure 11: X Resultant Forces

Figure 12: Z Resultant Forces
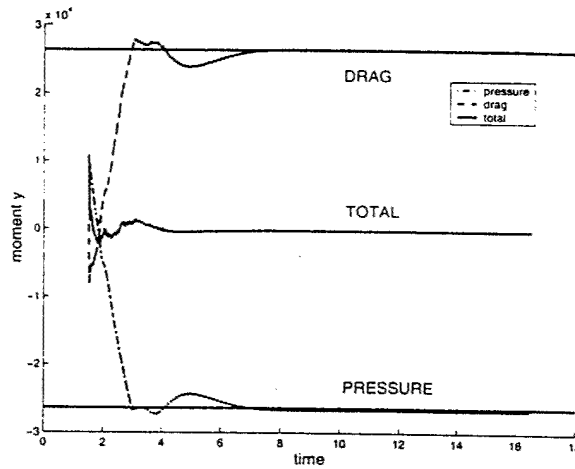
Figure 13: Y Resultant Moments
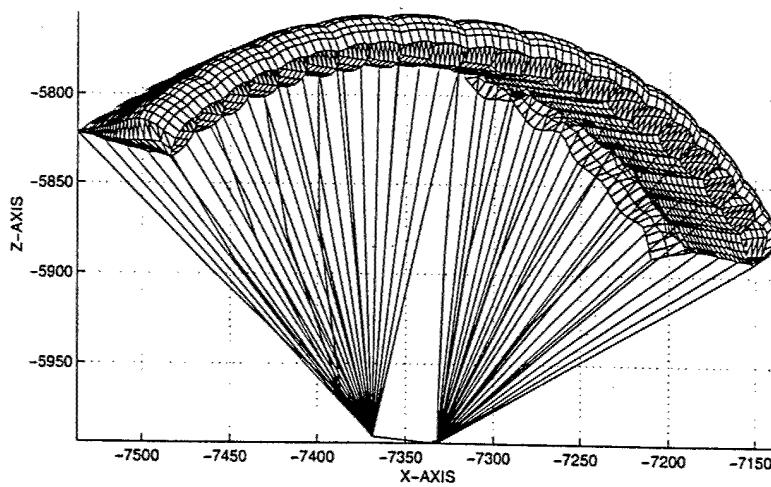
Figure 14: Parafoil During Turning Maneuver

7
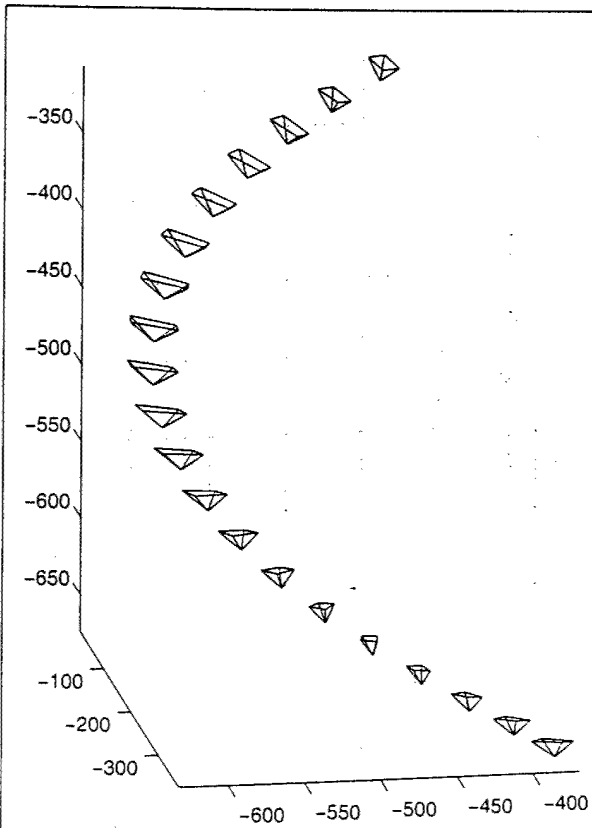
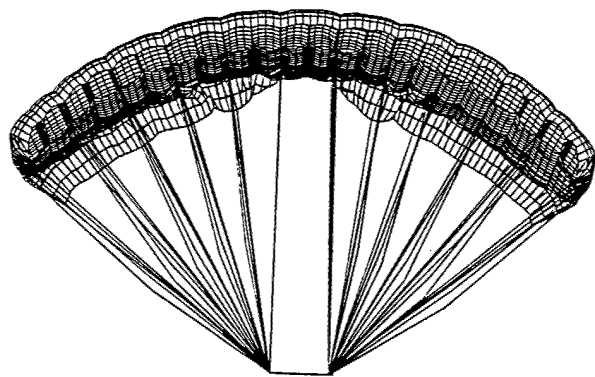Figure 15: Turning Trajectory of Parafoil

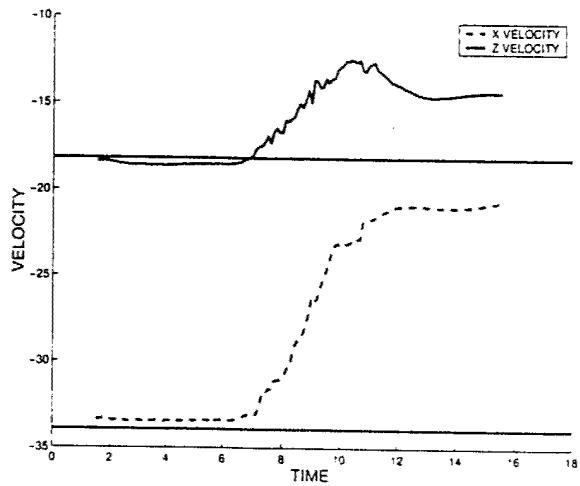Figure 16: Parafoil in Flare Configuration
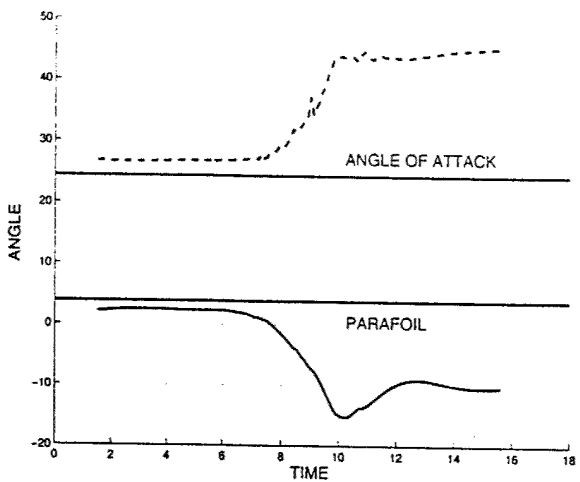

Figure 17: Velocities during Flare Maneuver

Figure 18: Parafoil Angle and Angle of Attack during Flare Maneuver

American Institute of Aeronautics and Astronautics